Proposal for a simulation method to determine the intraoperative torque load for pedicle screws with cellular functional areas

Franz Leonard Martin[1], Alexander Seidler[1,*], Kristin Paetzold-Byhain[1]

[1] Institute of Machine Elements and Machine Design, TUD Dresden University of Technology

Corresponding author:
Alexander Seidler
Chair of Virtual Product Development
George-Bähr-Straße 3c
01062 Dresden
☎ *+49351/46339138*
✉ *alexander.seidler@tu-dresden.de*

Abstract

Due to an ageing population and increased sedentary work, many back problems exist. Severe cases have to be stiffened by surgical therapies with screw-rod systems. However, due to the complex biomechanics of the spine, the screws implanted in the vertebrae often loosen. Additive manufacturing and new modeling methods mean complex lattice structures can now be designed for medical implants. This would make it feasible for the bone not only to grow onto the implant but even into it, thus improving the stiffness of the screw-bone bond and preventing premature loosening. However, this design poses a challenge to the design process of medical implants, as for screws with cellular-designed functional areas, the loads during implantation must be calculated. Therefore, all the calculation procedures were carried out in this work to predict intraoperative loads. For this purpose, the maximum torsional moment and the torsional moment curve were determined analytically according to Wilkie et al. and using explicit dynamic screw-implantation simulations and compared with experimental data. The analytical model showed an apparent overestimation of the torsional moment compared to the numerical model and the experimentally determined data. Based on this, a simulation process for calculating intra-operative loads during implantation and the feedback of the simulation data into the modeling was described.

Keywords

simulation, medical engineering, pedicle screw, cellular design

1. INTRODUCTION

In Germany, a high number of operations on the spine can be seen. Mainly older persons and especially women are affected [1]. For the surgical therapy of certain spinal disorders, such as scoliosis, herniated discs and vertebral bone fractures, screw-rod systems have established themselves as implants for permanent internal fixation. Despite the high reliability of the procedure, loosening of pedicle screws is a typical failure mechanism, especially in osteoporotic bone. [2, 3]

To improve the anchorage of pedicle screws in vertebral bone, the design of pedicle screws is a current focus in implant design research. In addition to other approaches that achieve an improvement through additional actuators or enlargement of the screw cross-sections, the use of cellular structures in implants is a promising approach to improving the anchoring of the implant to the bone. Here, the cellular structures represent a growth matrix for the bone, whereby the bone should grow optimally into the implant. This would enable tissue-sparing anchoring of pedicle screws in the vertebral bone. [4, 5]

However, inserting cellular structures leads to weakening the cross-section of screws (FIGURE 1). This weakening of the cross-section consequently affects the torsional stiffness of the bone screw. Accordingly, the implantation process represents the dominant load for the torsional loading of the cellular structures. Thus, the loads induced by the implantation process on the screw must be calculated to design the cellular structure.

Figure 1: Design of a gyroid structured poly-axial pedicle screw based on the design by Seidler et al. [5]

The current estimation of intraoperative torsional loads is done experimentally according to [6] and always requires prototypes. Therefore, there is currently no process for simulating intraoperative loads during the implantation of pedicle screws. The characterisation of the performance of bone screws is done by torsional strength (torsional yield strength, maximum torque, and breaking angle), insertion and removal torque, and pullout force [6]. Currently, the torsional strength of the screws can be predicted analytically, or the yield strength can be determined by static linear elastic finite element analysis (FEA). The pullout force can be expected in a simplified way using the equation described by [7]. The Chapman calculation is sufficient for FDA approval through the Safety and Performance Based Pathway 510(k) for regular bone screws [7, 8].

So far, the insertion torque (IT) is only experimentally determinable. However, there are analytical model descriptions by Seneviratne et al. [9] and Wilkie et al. [10]. The analytical description models represent extreme simplifications of reality and are well suited for estimating the IT in homogeneous materials. Nonlinearities of material properties and complex geometries represent the limits of the analytical model approach. Therefore, the use of analytical calculation models alone is insufficient for predicting the IT and the load analysis of bone screws.

The finite element method (FEM) is suitable for capturing such nonlinearities. This method is ideal for simulations of the implantation process of dental implants and osteosynthesis screws [11-14]. Here, mainly explicit simulations were used due to the strong deformations of the bone during the implantation of the bone screw. This type of FEM was used because of the stability advantages of high deformation/material failure and large-area complex contact. However, this specific solution method of FEM is characterised by a very long calculation time for fine FE meshes. The simulation's most minor time step is derived from the size of the smallest edge length used [11-14].

Therefore, this approach for the future design of cellular bone screws (Figure 1) does not seem suitable for these implants' design process. Since the design of implants with cellular-modified functional areas requires a product design with a high degree of novelty and the cellular structures significantly change the mechanical behaviour of the component, it is impossible to refer to existing data sets for the new development. For this purpose, methods for determining the driving torque of pedicle screws within the implantation process will be investigated in this study. This will allow future static mechanical simulations to design the cellular region of the bone screws based on the simulation process determined here. Therefore, this paper proposes a suitable simulation process to improve the design of redesigned medical implants with cellular-modified functional areas. The following research question is derived from this:

How can a suitable simulation process predict the intraoperative loading of bone screws with cellular design modification?

2. MATERIAL AND METHODS

Biomechanics of bone screw implantation

The torsional loading of the shaft of self-tapping bone screws depends on the driving torque due to implantation, which is composed of a thread-forming component of the tip and a friction component (Figure 2). According to Senerivatne et al. [9], the thread-forming part of the driving torque remains constant after an initial increase (Figure 2 Sec.1-3). In contrast, the frictional component increases due to increased thread surface area in engagement (Figure 2 Sec.4). When the screw disengages, the thread-forming moment decreases to zero, and the frictional moment reaches a constant value. Bone consists of a hard surface layer and loosened tissue inside the moment components can be determined separately for both layers and combined with the total load by superposition. Since the moments of resistance of the firmer marginal layer are higher, a cross-section of the screw may be loaded to the maximum when it enters this layer and experiences a lower torsional load after passing through the layer (Figure 2 Sec.5).
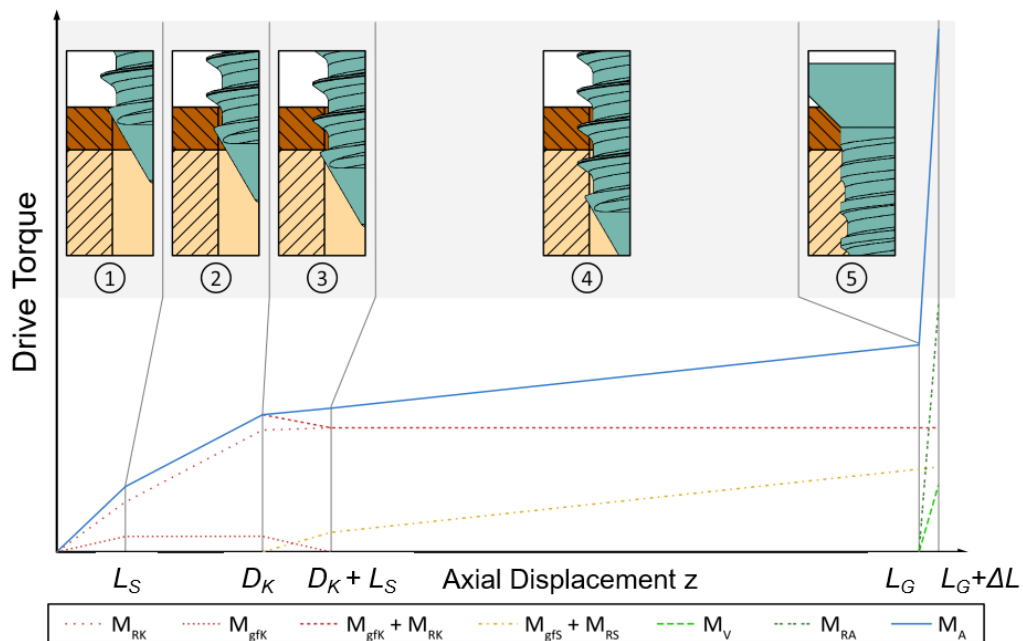
Figure 2: Progression of the driving torque during screwing through a cortical layer (brown) into cancellous bone (yellow). M_{RK}: frictional torque in cortical layer, M_{gfK}: thread-forming resistance torque in cortical layer, M_{RS}: frictional torque in cancellous bone, M_{gfS}: thread-forming resistance torque in cancellous bone, M_V: Preload torque, M_{RA}: friction torque of the head support, M_A: drive torque, L_{gfG}: axial length of the thread-forming geometry, D_k: layer thickness of the cortical bone, L_G: length of the thread, ΔL: preload travel.

To determine the maximum torsional load of a cross-section, the load at entry into the boundary layer is relevant, corresponding to the driving torque at this point. Therefore, a description of the progression of the driving torque is necessary.

Analytical design, according to Wilkie et al. [10]

The angle of rotation-torque relationship model from [10] was implemented in MatLab R2022b (The MathWorks Inc.). With the parametric description of *Eq.1* different thread forms can be modeled. The parameter representation $\vec{K}(t) = (r(t) \quad z(t))^T$ of the thread profile with the radial coordinate r(t) and the axial coordinate z(t) has been developed for the most common types of bone screws (Figure 3a), which describes the complete course of the profile (Figure 3b).

$$\vec{K}(t,\phi) = \begin{pmatrix} \hat{r}(t,\phi) \\ \hat{z}(t,\phi) \end{pmatrix} = \begin{pmatrix} \min\left(r(t), a \cdot z(t) + b \cdot (\phi + \phi_0)\right) \\ z(t) + \dfrac{\phi}{2\pi} P \end{pmatrix} \tag{1}$$

The parameter t runs in the limits [0,t_f]. The constants *a* and *b* are calculated from the opening angle of the tip and the thread pitch *P*. ϕ describes the angle of rotation around the screw axis.

A description for typical bone screw thread types HA and HB according to [15] was derived manually (Figure 3a). The model assumes ductile, homogeneous, isotropic material. The solution is numerical. For code verification, the screws HA4.5 and HB6.5 curves according to [15] from [10] were reproduced with the given parameters. Missing parameters of the thread geometry were taken from [15]. A sensitivity analysis was performed to ensure the numerical solution was sufficiently independent of the discretisation. The model was then parameterised to calculate the torque curve of the experimental test setup (Figure 4) with measured values of the thread, the compressive strength of the test specimen, and a coefficient of friction of 0.2.

a)   b)
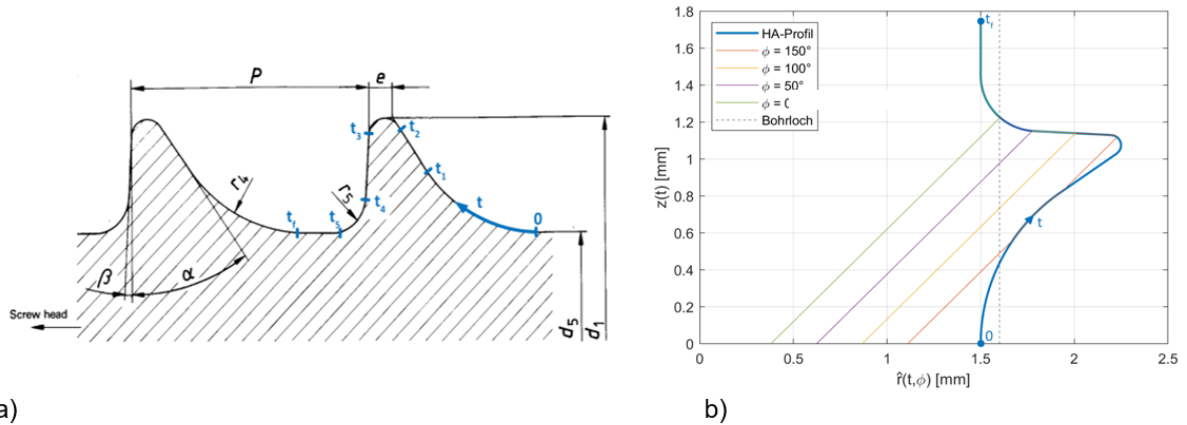
Figure 3: a) Dimensions of a HA thread [6]; b) Parametric description of the thread profile

Implicit simulation

Modeling the implantation process using static or implicit dynamic methods is conceivable. However, the high deformations and large-scale contact lead to a strong non-linearity of the problem, so iterative equation solvers converge poorly or not at all under very high numerical effort, also Dorogoy et al. reported in their study about convergence issues that led to the dropping of the approach [12].

Explicit simulation

To evaluate the suitability of explicit dynamic FEM a simulation model was built in *Ansys Workbench R2023a Explicit Dynamic*. This modeled the experimental test setup described in [6]. The screw was modeled with the measured dimensions of a total length of 45mm, an outer diameter of 7.5 mm and a pitch of 2.8 mm of a HA-Thread. The head geometry was neglected, and the thread tooth's radius was removed for better meshing. The screw was meshed as a rigid body with a surface mesh of 188 linear triangular elements and 32545 linear quadrilateral elements with a target size of 0.2 mm. In order to reduce the calculation area, a cylindrical section of the test specimen was considered, which includes the influence zone of the thread forming process (diameter 15 mm, length 28 mm, centrically pre-drilled with diameter 5.5 mm). This was meshed with 114576 linear reduced integration hexahedral elements. The inner zone near the implant up to a diameter of 8.5 mm was finely cross-linked with an edge length of 0.15 mm in the axial and radial direction and 0.4 mm along the circumference. The reduction in calculation effort justifies the decrease in element quality.

The specimen material was modeled homogeneously and isotropically. Linear elastic-plastic material behaviour with a modulus of elasticity of 23 MPa [16] was modelled. The apparent Poisson ratio was estimated to be 0.3 [17]. A linear plasticity model with the von-Mises yield criterion has been used to model the stress-strain-behaviour of rigid polyurethane foams under compressive loading conditions. The yield strength was approximated by the compressive strength (2.3 MPa) [16]. Hardening has been introduced with a tangent modulus of 1/1000*E (23 kPa) for numerical purposes, which leads to almost ideal-plastic behaviour. The instantaneous material failure occurred when the first principal strain reached a failure strain of 12%, resulting in element deletion. Failure strain is not the same as the engineering strain at failure, as this does not consider the necking at the fracture. Therefore, an iterative/experimental determination of the parameter is necessary.

The typical modulus of elasticity and strengths of titanium are much higher than those of the test specimen. Therefore, deformations do not have to be considered if the torsional moment does not exceed the yield strength of the screw. The screw was modeled as a rigid body, as these do not influence the simulation's stable time increment; thus, acceptable time increments are achieved even with the fine meshing of the screw.

The cut surfaces of the specimen were clamped (FIGURE 4 blue) to account for the support effect of the surrounding material. The screw was rigidly supported concerning the global coordinate system. The feed and angular velocity of the experiment were scaled by a factor and imposed on the degrees of freedom of the z-axis (FIGURE 4 red). All other degrees of freedom are constrained. A penalty contacts with a friction coefficient of 0.4 was defined between the inner circular ring and the screw.

The Simulation was done with an element size of 0.14x0.14x0.3 mm, velocity scaling with a factor of 200, a mass scaling with a factor of 7.88. The failure strain was 12%, and three friction coefficients, 0.2, 0.3, and 0.4, were checked to find the best match with the experimental data.
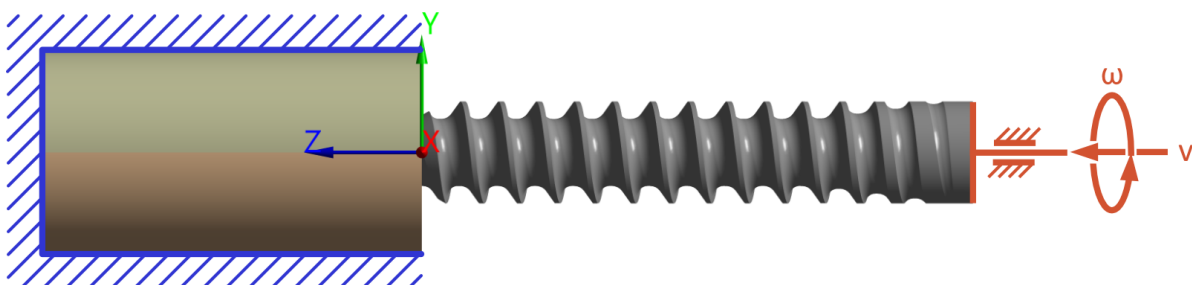
Figure 4: FE-Model for explicit load analysis on bone screws

Experimental setup

Experimental measurements were carried out to validate the process flow. The experimental setup (Figure 5c) is based on [6]. A commercially available pedicle screw (Medtronic CD Horizon™ Spinal System, Fixed angle Screw for 5.5 mm Rod, 7. 5 x 45 mm) (Figure 5a) made of a medical titanium alloy was screwed five times vertically into cube-shaped, centrically predrilled test specimens (edge length 40±5 mm, hole diameter 5.5 mm) (Figure 5b) made of cellular rigid polyurethane foam (SawBones® Cellular Rigid Polyurethane Foam, apparent density 10 pcf (160 kg/m^3)) [16]. In contrast to [6], the screw was clamped in a four-jaw chuck. The specimen was aligned by probing the drill hole and then fixed. The screw was inserted at a constant angular speed of 30 rpm. The steady feed rate of 1.4 mm/s corresponded to the thread pitch. The screw-in depth was 21 mm.

The angle of rotation, axial displacement, axial force, and drive torque were recorded at a sampling rate of 100 Hz. The axial force did not exceed 30 N. The approximately linear torque-angle relationship increase was evaluated using linear regression over seven full revolutions. The first 20 measured values were truncated due to overlap with disturbance variables.
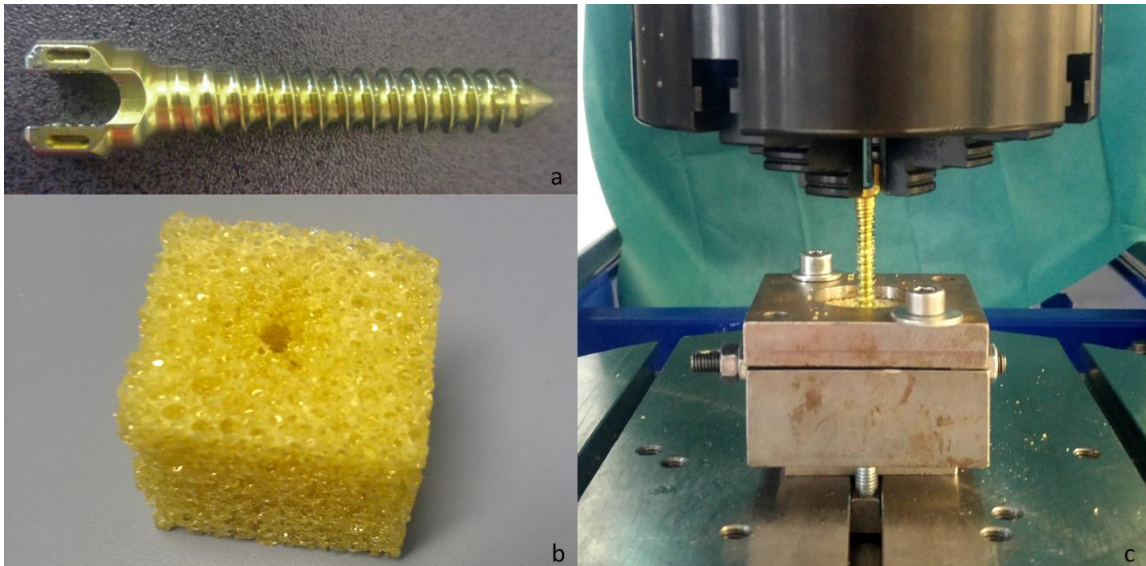
Figure 5: a) Pedicle screw from Medtronic CD Horizon™ Spinal System; b) Predrilled block of sawbones;
c) Experimental Setup of the medicon pedicle screw in saw bones;

3. RESULTS AND DISCUSSION

The drive torque of the Medtronic pedicle screw was determined using the simulations and the described experimental set-up and then compared with each other. For this purpose, equivalent CAD models were built for the simulations. FIGURE 4 shows the torsional moment over the number of complete rotations of the screw in the bone or artificial bone. Because no plausible zero point of the torsional moment could be determined in the experiments because of internal errors in the testing machines, the maximum torsional moment, as well as the slope of the torsional moment, is evaluated over the screw-in depth ("number of turns of the screw").

For the analytical approach, the torsional moment was calculated with a friction value of 0.2 (Figure 6 purple). The curve shows a nearly linear relationship between the number of rotations and the drive moment after the development of the thread forming component. With a drive moment slope of $217*10^{-3}$ Nmm/° and a maximum torsional moment after seven revolutions of 510 Nmm.

Three different friction values were determined for the explicit FEM. The slope of the moment curve with a friction coefficient of 0.2 (FIGURE 6 yellow) is $19.8*10^{-3}$ Nmm/° and a maximum value of approx. 60 Nmm. The slope of the torque curve with a coefficient of friction

of 0.3 (Figure 6 red) is 33.8*10^{-3} Nmm/° and a maximum torque of 95 Nmm. The coefficient of friction of 0.4 with the same simulation set-up results in a slope of 46.3*10^{-3} Nmm/° and a maximum torque of 115 Nmm.

The five measurements of the experimental investigation show an approximately linear relationship between torque and angle of rotation. The mean increase is 34.1*10^{-3} Nmm/° (SD 6.84*10^{-3} Nmm/°), and the maximum torque is 95Nmm.

Based on this data, the individual simulation variants can be compared according to their suitability for determining the occurring intraoperative loads. An apparent deviation between the experiments and the analytical calculation can already be seen (Figure 6). The slope of the torsional moment curve is already more significant than that of the experimental data by a factor of 6.85. This means that the maximum drive torque after 7 turns also deviates by a relative factor of 540%. In contrast, the slope of the simulation's torque curve corresponds to a friction value of 0.3, corresponding to that of the experimental data.
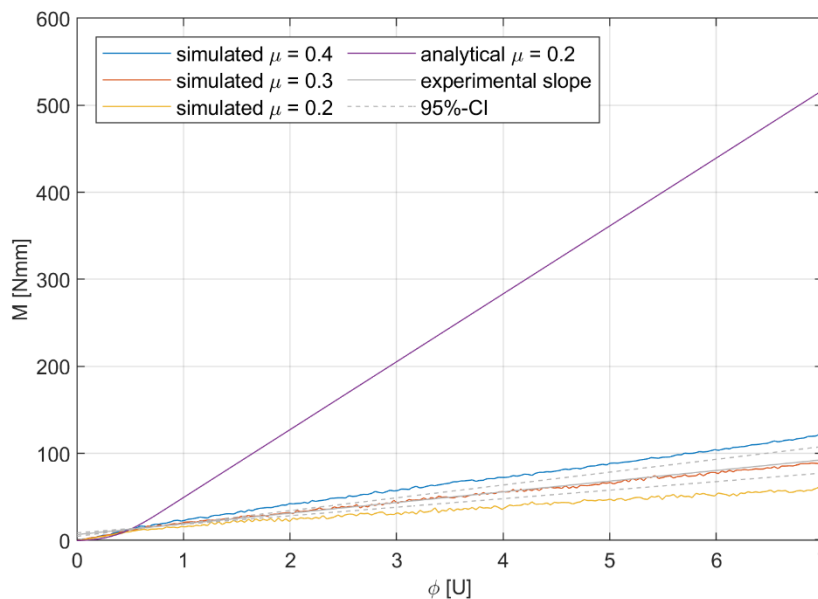
Figure 6: Drive torque curve over the number of revolutions

These results show that the analytical approach of Wilkie et al. [10] shows acceptable deviations in the range of the first half turn. After that, the deviation from the experimental data and the simulation results increases significantly. In contrast, the simulation results show a significantly smaller deviation than the experimental data. The torsional moment curve at an assumed friction value of 0.3 corresponds to the experimentally determined torque curve.

The significant deviation from the analytical model can be attributed to the fact that the model has its limits with non-linear material properties. In addition, the highly simplified pressure models between screw and bone can also lead to an overestimation of the torque moment since, in reality, the bone tissue is an open-porous material in which the pressure conditions between the implant and the bone change stochastically. Accordingly, this approach is unsuitable for the concrete design of modified pedicle screws with cellular functional areas. However, the method shows potential for the conceptual phase of the cellular structures for the design of the functionally structured areas and the dimensional estimation of the bone screw for cellular modification. However, correction factors should be developed in the future to reduce the large deviations. In contrast, nonlinearities can be better implemented in the explicit dynamic FEA, again using a homogenisation approach for material modeling. The explicit dynamic model's deviations noticeably depend on the selected friction coefficient between the screw and the bone. This can only be determined retrospectively via experimental validation. Accordingly, one is dependent on experimental comparative measurements for an

accurate simulation. However, this approach has a significantly more accurate prediction potential than the analytical solution.

The following conclusions can be drawn from these analyses for developing a simulation process flow to design bone screws with a cellular structured functional area. Even if the analytical model estimates the torsional loads during implantation significantly higher, this approach is suitable for finding the appropriate cellular structure, since the significantly faster calculation times can ensure a higher dynamic in the development process. In contrast, the calculation of the intraoperative loads using explicit dynamic FEA has a significantly higher degree of accuracy with simultaneously higher calculation times. Therefore, this method is suitable for design and load-adaptive geometry modification.

As a result of the numerical investigations, the following simulation process (Figure 7) was developed to design cellular bone screws. Here, the geometric model of the screw is realised via a field description in the software *nTopology*. This geometric description is a prerequisite for the geometric representation of the cellular bone screw. Based on this, it depends on the development stage of the design process whether a load assumption with linear geometry and material properties or a non-linear load assumption should be calculated. According to Wilkie et al. [10], the linear load assumption is suitable for the pre-selection and design determination of the geometric structures, as rough design adjustments are possible in short iteration loops.

However, the non-linear load assumption determination shows its advantages in the concrete structural design of cellular structures. Subsequently, the drive torque occurring at the bone screw during implantation is determined with the respective model approach and transferred to a static-mechanical FEM as a boundary condition. The static-mechanical analysis is then used to determine the stresses in the bone screw. The occurring stresses are then analysed, and a decision is made as to whether the cellular structure can withstand the theoretical intraoperative loads. If critical areas in the cellular structure are determined in the analysis, feedback from the simulation results in the geometry model represented by fields. Here, the Von Mises stress distribution is fed back into the software *nTopology* using a csv-file and represented by a field description. On this basis, the solution variables are converted into geometry-manipulating control variables, and the structure is adjusted in the critical areas, e.g., by thickening the bars. If the stress distribution in the component corresponds to the defined loads, the geometry model can be prepared for manufacturing using additive manufacturing.
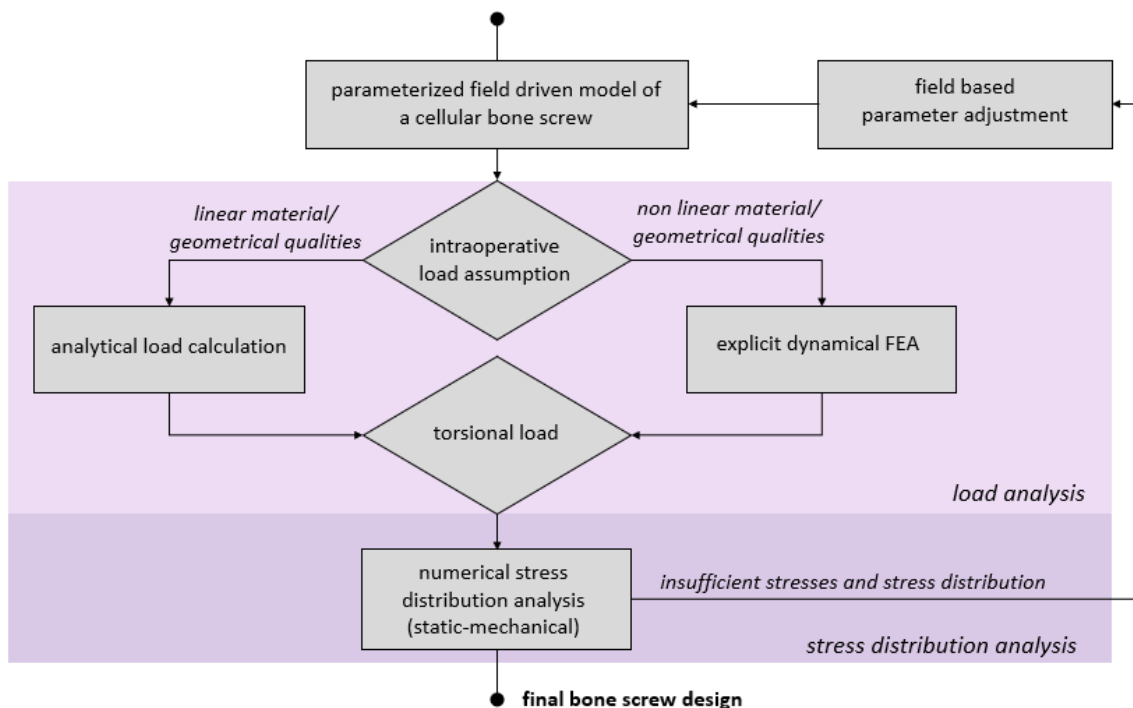
Figure 7: Simulation process for load adaptive cellular bone screw design

4. CONCLUSION

This paper set up a simulation process to support the future design of bone screws with cellularly designed functional areas. The simulation focused on calculating the torsional loading of the bone screws during implantation, using this for less complex static-mechanical simulation on torque-induced stress analysis. Since these loads have been of little relevance in the design of conventional bone screws, an extensive literature search was conducted to determine all approaches for calculating the intraoperative loads on bone screws during implantation. The result of the literature search showed that the intraoperative loads could be determined either via an analytical model approach, according to Wilkie et al. [10], or via explicit FEM [11-13]. Based on this, both model approaches were tested on a representative example, whereby certain model limits of the two approaches were also revealed in terms of accuracy. Based on these simulation results, a process for designing bone screws with cellular functional areas was established.

In future studies, the model of Wilkie et al. [10] should be investigated for its extensibility to nonlinear material models in order to realise a higher prediction accuracy with this model. Furthermore, the complete validation of the simulation process for generating bone screws with cellular-modified functional areas is still pending.

ACKKNOWLEDGMENT

REFERENCES

[1] Tesch F, Lange T, Dröge P et al. Indication for spinal surgery: associated factors and regional differences in Germany. BMC Health Serv Res; DOI: 10.1186/s12913-022-08492-3

[2] Heck VJ, Klug K, Prasse T et al. Projections From Surgical Use Models in Germany Suggest a Rising Number of Spinal Fusions in Patients 75 Years and Older Will Challenge Healthcare Systems Worldwide. Clin Orthop Relat Res; DOI: 10.1097/corr.0000000000002576

[3] Kater EP de, Sakes A, Edström E et al. Beyond the pedicle screw-a patent review. European spine journal: official publication of the European Spine Society, the European Spinal Deformity Society, and the European Section of the Cervical Spine Research Society; DOI: 10.1007/s00586-022-07193-z

[4] Werner M, Hammer N, Rotsch C et al. Experimental validation of adaptive pedicle screws-a novel implant concept using shape memory alloys. Med Biol Eng Comput; DOI: 10.1007/s11517-019-02059-x

[5] Seidler A, Mehlhorn L, Sembdner P et al. Proposal for an Adaptive Bone Screw Design Based on FEA Studies Exemplified by Pedicle Screw. In: Volume 3A: 47th Design Automation Conference (DAC). American Society of Mechanical Engineers; DOI: 10.1115/DETC2021-67768; 2021

[6] ASTM International. Standard Specification and Test Methods for Metallic Medical Bone Screws; (ASTM F543-17), 2017

[7] Chapman JR, Harrington RM, Lee KM et al. Factors affecting the pullout strength of cancellous bone screws. Journal of biomechanical engineering; DOI: 10.1115/1.2796022

[8] US Food and Drug Administration. Orthopedic Non-Spinal Metallic Bone Screws and Washers – Performance Criteria for Safety and Performance Based Pathway: Guidance for Industry and Food and Drug Administration Staff (11.12.2019). Internet: www.fda.gov/media/130866/download; Date: 07.07.2023

[9] Seneviratne LD, Ngemoh FA, Earles SWE et al. Theoretical modelling of the self-tapping screw fastening process. Proceedings of the Institution of Mechanical Engineers, Part C: Journal of Mechanical Engineering Science 2001; 215C: 135–154

[10] Wilkie J, Docherty PD, Stieglitz T et al. Geometric Generalization of Self Tapping Screw Insertion Model. Annu Int Conf IEEE Eng Med Biol Soc; DOI: 10.1109/EMBC46164.2021.9630157

[11] Affes F, Ketata H, Kharrat M et al. How a pilot hole size affects osteosynthesis at the screw-bone interface under immediate loading. Med Eng Phys; DOI: 10.1016/j.medengphy.2018.07.002

[12] Dorogoy A, Rittel D, Shemtov-Yona K et al. Modeling dental implant insertion. J Mech Behav Biomed Mater; DOI: 10.1016/j.jmbbm.2017.01.021

[13] Ketata H, Affes F, Kharrat M et al. A comparative study of tapped and untapped pilot holes for bicortical orthopedic screws - 3D finite element analysis with an experimental test. Biomed Tech (Berl); DOI: 10.1515/bmt-2018-0049

[14] Ovesy M, Indermaur M, Zysset PK. Prediction of insertion torque and stiffness of a dental implant in bovine trabecular bone using explicit micro-finite element analysis. J Mech Behav Biomed Mater; DOI: 10.1016/j.jmbbm.2019.06.024

[15] ISO Internationale Organisation für Normung. Implants for surgery - Metal bone screws with hexagonal drive connection, spherical under-surface of head, asymmetrical thread - Dimensions; (ISO 5835). Zürich, Wien, Berlin: Beuth Verlag GmbH, 1991

[16] Sawbones. Biomechanical test materials and composite bones for test and validation studies: Biomechanical Products Catalogue (15.02.2021). In the Internet: www.sawbones.com/media/assets/product/documents/biomechanical_catalog2021.pdf; Date: 13.06.2023

[17] Rinde JA. Poisson's ratio for rigid plastic foams. J. Appl. Polym. Sci.; DOI: 10.1002/app.1970.070140801